Synthesis and Characterization of Poly(fluorene-*co*-*alt*-phenylene) Containing 1,3,4-Oxadiazole Dendritic Pendants

CHUNG-WEN WU, HSIAO-HSIEN SUNG, HONG-CHEU LIN

Department of Materials Science and Engineering, National Chiao Tung University, Hsinchu, Taiwan, Republic of China

Received 7 April 2006; accepted 3 August 2006
DOI: 10.1002/pola.21720
Published online in Wiley InterScience (www.interscience.wiley.com).

ABSTRACT: A series of poly(fluorene-*co*-*alt*-phenylene)s containing various generations of dendritic oxadiazole (OXD) pendent wedges were synthesized by the Suzuki polycondensation of OXD-functionalized 1,4-dibromophenylene with 9,9-dihexylfluorene-2,7-diboronic ester. The obtained polymers possessed excellent solubility in common solvents and good thermal stability. Photophysical studies showed that the dendronized polymers appended with higher generations of OXD dendrons exhibited enhanced photoluminescence efficiencies and narrower values of the full width at half-maximum. This was attributed to the shielding effect induced by the bulky dendritic OXD side chains, which prevented self-quenching and suppressed the formation of aggregates/excimers. The energy transfer from the OXD dendrons to the polymer backbones was very efficient when excitation of the peripheral OXD dendrons resulted mainly in the polymer backbone emission alone. In particular, the photoluminescence emission intensities by the sensitized excitations of OXD dendrons in solid films of the polymers were all stronger than those by the direct excitations of their polymer conjugated backbones. © 2006 Wiley Periodicals, Inc. J Polym Sci Part A: Polym Chem 44: 6765–6774, 2006

Keywords: dendrimers; dendritic pendant; dendronized polymers; energy transfer; oxadiazole (OXD); polyfluorene

INTRODUCTION

Organic light-emitting diodes (OLEDs) have the potential to achieve low-cost and full-color flat-panel displays because of their high brightness, easy fabrication, and wide range of emission colors.[1,2] However, some important and fundamental challenges remain unsolved, including the maximization of external quantum efficiencies (EQEs), the design and synthesis of new materials with purer colors, and modes of addressing devices for a full-color display with optimized resolution. A major factor responsible for low device EQEs is that the charge (electron and hole) injection and transportation in emissive materials are generally unbalanced. In general, most electroluminescent polymers inject and transport holes more efficiently than electrons because of their inherent richness of π electrons. One approach for improving the electron-transport properties of polymers is to incorporate electron-deficient segments into main chains[3–5] or as pendants attached to the backbones.[6–10] Oxadiazole (OXD) units are among the most widely investigated electron-transport structures for OLEDs because of the high electron affinity of the OXD segments in OLED molecules. Several OXD-containing light-emitting polymers have also been prepared in recent years.[11–13]

This article includes Supplementary Material available from the authors upon request or via the Internet at www.interscience.wiley.com/jpages/0887-624X/suppmat

Correspondence to: H.-C. Lin (E-mail: linhc@cc.nctu.edu.tw)

Journal of Polymer Science: Part A: Polymer Chemistry, Vol. 44, 6765–6774 (2006)

Dendronized polymers may exhibit superior properties in future applications in comparison with their nondendronized analogues for a number of reasons. The dendritic side chains, acting as solubilizers, can enhance processability without the loss of mechanical or thermal stability provided by the rigid polymer backbones. The dense dendron decorations may provide efficient shields, such as protection against chemical reactants and prevention of molecular aggregation. In addition, the dendrons may serve, depending on their chemical nature, as light-harvesting antennae, charge carriers, and so on.[14]

Polyfluorenes (PFs) have attracted a great deal of attention because of their excellent thermal and chemical stability as well as high photoluminescence (PL) quantum efficiencies.[15–18] However, the problems encountered with PFs in general are their tendency to aggregate and form excimers, which lead to blue-green emissions with fluorescence quenching. In previous reports, research regarding PFs appended with polyphenylene dendrons[19,20] or Fréchet-type dendrons[21–23] demonstrated that the shielding effect provided by the dendritic side chains on the conjugated backbones of PFs suppresses the formation of aggregates/excimers. Recently, Bo et al.[24] first reported the synthesis of dendronized PFs containing functional carbazole dendrons, with their focal benzyl groups directly bonded to the C-9 carbon of the fluorene units. The copolymerization approach has been widely used in the preparation of conjugated polymers to achieve specific electronic and physical properties. It has also been demonstrated that the copolymerization of fluorenes with various aryl partners allows for the tunability of the electronic properties with enhanced stability.[25–27]

In hopes of combining both excellent electron affinities and energy-transfer (light-antenna) properties in polymers, a new family of polyfluorene-*co*-*alt*-phenylenes carrying peripheral OXD functional dendrons attached to the 2- and 5-positions of the phenylene rings is presented in this report. Thus, the dendritic wedges play the roles of efficient site isolation and excellent electron affinity. In particular, the enhanced PL emission properties of dendronized polymers have been observed in contrast to those of analogous conjugated main chains without dendritic pendants, for which similar PFs (lacking alternative phenylene backbones) containing different generations of poly (benzyl ether) dendritic wedges with OXD peripheral functional groups have also been reported recently.[28] Therefore, the light harvest of chromophores from the luminescence of the dendritic pendants by the light-antenna design is more efficient than direct excitation at the maximum absorption of light-emitting segments by an external light source.

EXPERIMENTAL

Characterization

^{1}H NMR spectra were recorded on a Varian Unity 300-MHz spectrometer with $CDCl_3$ as the solvent. Elemental analyses were performed on a Heraeus CHN-OS rapid elemental analyzer. Monomers **M1**–**M3** (**4**–**6**) were characterized with ^{1}H NMR, elemental analyses, and fast atom bombardment [FAB; or matrix-assisted laser desorption/ionization time-of-flight (MALDI-TOF)] mass spectrometry (MS). Transition temperatures were determined with differential scanning calorimetry (DSC; Diamond model, PerkinElmer) at a heating and cooling rate of 10 °C/min. Thermogravimetric analysis (TGA) was conducted on a DuPont Thermal Analyst 2100 system with a TGA 2950 thermogravimetric analyzer at a heating rate of 20 °C/min. Gel permeation chromatography (GPC) analysis was conducted on a Water 1515 separation module with polystyrene as a standard and tetrahydrofuran (THF) as an eluant. Ultraviolet–visible (UV–vis) absorption spectra were recorded in dilute chloroform solutions (10^{-6} M) on an HP G1103A spectrophotometer, and fluorescence spectra were obtained on a Hitachi F-4500 spectrophotometer. Polymer solid films were spin-coated on quartz substrates from THF solutions with a concentration of 10 mg/mL. Cyclic voltammetry measurements of the polymer films were performed on a BAS 100 B/W electrochemical analyzer in acetonitrile with 0.1 M tetrabutylammonium hexafluorophosphate as the supporting electrolyte at a scanning rate of 100 mV/s. A polymer film on a glassy carbon disk electrode was used as the working electrode. A platinum wire was used as the counter electrode, and a silver wire was used as the reference electrode. All preparations and measurements were carried out at room temperature under nitrogen. The potentials were measured against a Ag/Ag^+ (0.01 M $AgNO_3$) reference electrode with ferrocene as the internal standard. The onset potentials were determined by the intersection of two tangents drawn at the rising current and background current of the cyclic voltammogram.

Materials

2,7-Bis(4,4,5,5-tetramethyl-1,3,2-dioxaborolane-2-yl)-9,9-dihexylfluorene (**M4**) was synthesized according to literature procedures.[29] The synthesis and characterization of compounds **1**–**3** and their intermediates are described in the supplemental material. The chemicals and solvents were reagent-grade and were purchased from Aldrich, Acros, TCI, and Lancaster Chemical Co. Dichloromethane and THF were distilled to remain anhydrous before use, and the other chemicals were used without further purification.

General Synthetic Procedure for Dendronized Monomers M1–M3 (4–6)

A mixture of corresponding compound **1**, **2**, or **3** (2.1 equiv), 2,5-dibromobenzene-1,4-diol (1 equiv), K_2CO_3 (2.5 equiv), and 18-crown-6 (0.2 equiv) in dry THF was heated to refluxing and stirred under nitrogen for 48 h. The mixture was evaporated to dryness under reduced pressure, and the residue was partitioned between water and CH_2Cl_2. The aqueous layer was extracted with CH_2Cl_2, and the organic layers were dried over $MgSO_4$. The crude product was purified as outlined in the following text.

M1 (4)

Monomer **M1** (**4**) was purified by column chromatography with EA/CH_2Cl_2 (1:10) to obtain a white solid.

Yield: 75%. ^{1}H NMR (ppm, $CDCl_3$): 0.90–0.97 (m, 12H), 1.34–1.54 (m, 16H), 1.75–1.77 (m, 2H), 3.92 (d, 4H), 5.16 (s, 4H), 7.03 (d, 4H), 7.21 (s, 2H), 7.63 (d, 4H), 8.06 (d, 4H), 8.16 (d, 4H). Elem. Anal. Calcd. for $C_{52}H_{56}Br_2N_4O_6$: C, 62.91%; H, 5.69%; N, 5.64%. Found: C, 63.01%; H, 5.73%; N, 5.64%. MS (FAB): *m/z* [M^+] 993.20, calcd. *m/z* 992.83.

M2 (5)

Monomer **M2** (**5**) was purified by column chromatography with EA/CH_2Cl_2 (1:6) to obtain a white solid.

Yield: 78%. ^{1}H NMR (ppm, $CDCl_3$): 0.91–0.97 (m, 24H), 1.35–1.55 (m, 32H), 1.72–1.78 (m, 4H), 3.92 (d, 8H), 5.01 (s, 4H), 5.14 (s, 8H), 6.58 (s, 2H), 6.70 (s, 4H), 7.01 (d, 8H), 7.09 (s, 2H), 7.57 (d, 8H), 8.05 (d, 8H), 8.13 (d, 8H). Elem. Anal. Calcd. for $C_{112}H_{120}Br_2N_8O_{14}$: C, 68.56%; H, 6.16%; N, 5.71%. Found: C, 68.91%; H, 6.27%; N, 5.80%. MS (MALDI-TOF): *m/z* [M^+] 1962.84, calcd. *m/z* 1962.00.

M3 (6)

Monomer **M3** (**6**) was purified by column chromatography with EA/CH_2Cl_2 (1:12 gradually increasing to 1:8) to obtain a white solid.

Yield: 65%. ^{1}H NMR (ppm, $CDCl_3$): 0.91–0.96 (m, 48H), 1.25–1.54 (m, 64H), 1.70–1.76 (m, 8H), 3.89 (d, 16H), 4.96 (s, 4H), 4.99 (s, 8H), 5.08 (s, 16H), 6.50 (s, 2H), 6.54 (s, 4H), 6.65 (s, 4H), 6.66 (s, 8H), 6.99 (d, 16H), 7.06 (s, 2H), 7.53 (d, 16H), 8.02 (d, 16H), 8.08 (d, 16H). Elem. Anal. Calcd. for $C_{232}H_{248}Br_2N_{16}O_{30}$: C, 71.44%; H, 6.41%; N, 5.75%. Found: C, 71.34%; H, 6.50%; N, 5.76%. MS (MALDI-TOF): *m/z* [M^+] 3900.28, calcd. *m/z* 3900.35.

General Synthetic Procedure for Dendronized Polymers P1–P3

A mixture of corresponding dendritic monomer **M1**, **M2**, or **M3** (**4**, **5**, or **6**), **M4**, K_2CO_3, toluene, and H_2O was degassed, and Pd[P(*p*-tolyl)$_3$]$_3$ was added under a nitrogen atmosphere. The reaction mixture was heated to refluxing and stirred under nitrogen for 48 h. End-group capping was performed through the heating of the solution under refluxing for 6 h sequentially with phenylboronic acid and iodobenzene. After cooling, the crude polymers were dissolved in THF and purified by precipitation from methanol, and dendronized polymers **P1**–**P3** were collected and dried *in vacuo*.

Dendronized Polymer P1

M4 (273.5 mg, 0.46 mmol), **M1** (**4**; 463 mg, 0.46 mmol), K_2CO_3 (1.1 g), Pd[P(*p*-tolyl)$_3$]$_3$ (8.00 mg), toluene (10 mL), and H_2O (4 mL) were used in the reaction mixture. Polymer **P1** was obtained as a slightly yellow solid.

Yield: 75%. ^{1}H NMR (ppm, $CDCl_3$): 0.62–0.97 (m, 34H), 1.26–1.75 (m, 22H), 3.90 (d, 4H), 5.16 (s, 4H), 7.00 (d, 4H), 7.20 (s, 2H), 7.49 (d, 4H), 7.63 (broad, 4H), 7.83 (d, 2H), 8.03 (d, 4H), 8.09 (d, 4H). Elem. Anal. Calcd. for $(C_{77}H_{88}N_4O_6)_n$: C, 79.35%; H, 7.61%; N, 4.81%. Found: C, 78.12%; H, 7.56%; N, 4.45%.

Dendronized Polymer P2

M4 (120 mg, 0.20 mmol), **M2** (**5**) (400 mg, 0.20 mmol), K_2CO_3 (1.1 g), Pd[P(*p*-tolyl)$_3$]$_3$ (8.00 mg), toluene (10 mL), and H_2O (4 mL) were used in the

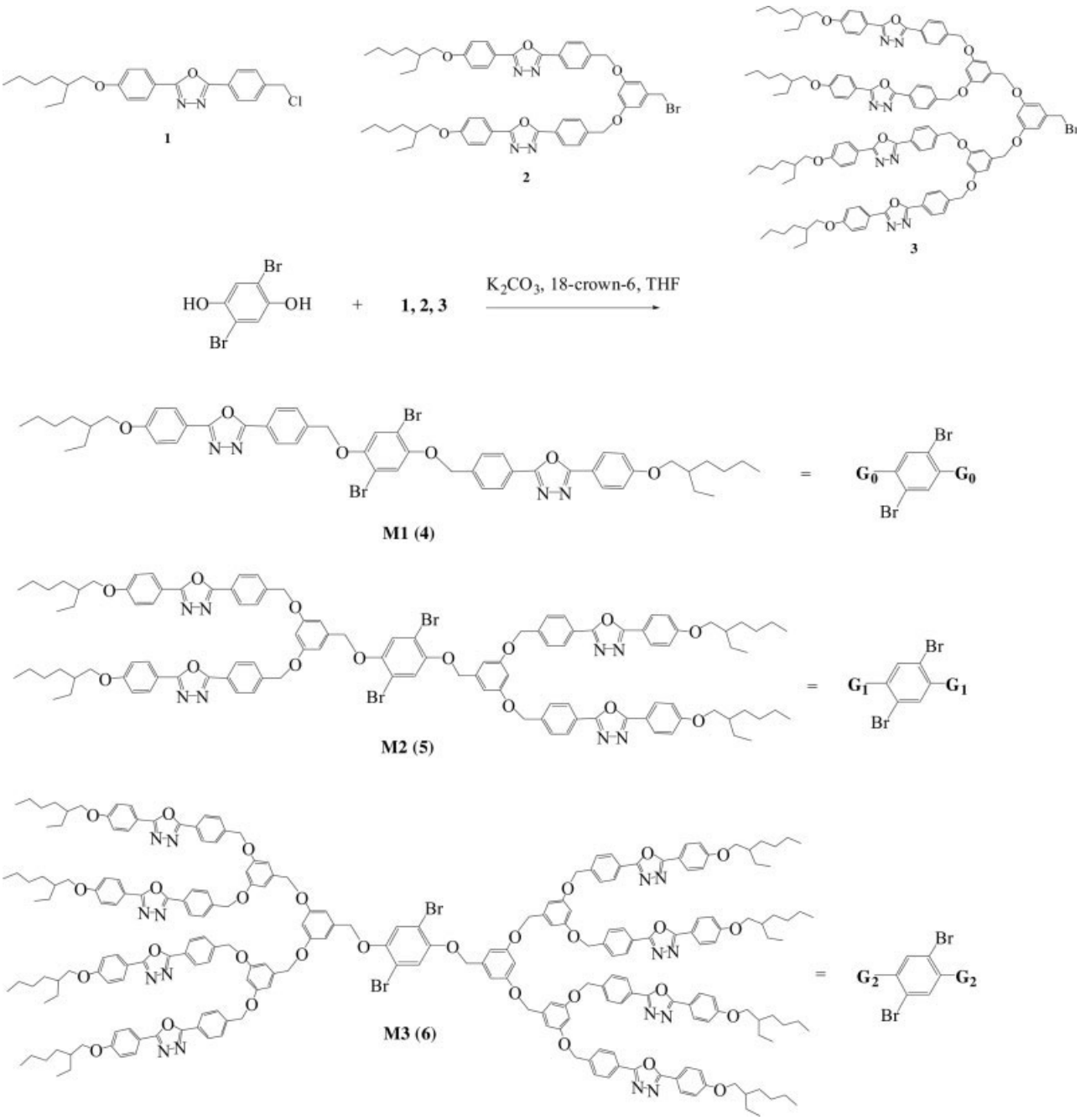

Scheme 1. Synthetic routes of monomers **M1**–**M3**.

reaction mixture. Polymer **P2** was obtained as a slightly yellow solid.

Yield: 68%. ^{1}H NMR (ppm, $CDCl_3$): 0.63–0.97 (m, 46H), 1.31–1.73 (m, 40H), 3.84–3.92 (broad, 8H), 4.89 (s, 8H), 5.10 (broad, 4H), 6.46 (s, 2H), 6.61 (s, 4H), 6.93–7.03 (broad, 10H), 7.42 (d, 8H), 7.74 (broad, 6H), 7.97–8.14 (broad, 16H). ELEM. ANAL. Calcd. for $(C_{137}H_{152}N_8O_{14})_n$: C, 77.08%; H, 7.18%; N, 5.25%. Found: C, 75.99%; H, 7.17%; N, 4.67%.

Dendronized Polymer P3

M4 (60 mg, 0.10 mmol), **M3** (**6**) (400 mg, 0.10 mmol), K_2CO_3 (1.1 g), Pd[P(*p*-tolyl)$_3$]$_3$ (8.00 mg), toluene (10 mL), and H_2O (4 mL) were used in the reaction mixture. Polymer **P3** was obtained as a slightly yellow solid.

Yield: 70%. ^{1}H NMR (ppm, $CDCl_3$): 0.63–0.95 (m, 70H), 1.29–1.66 (m, 72H), 3.80–3.89 (broad, 16H), 4.88 (broad, 28H), 6.44–6.59 (broad, 18H),

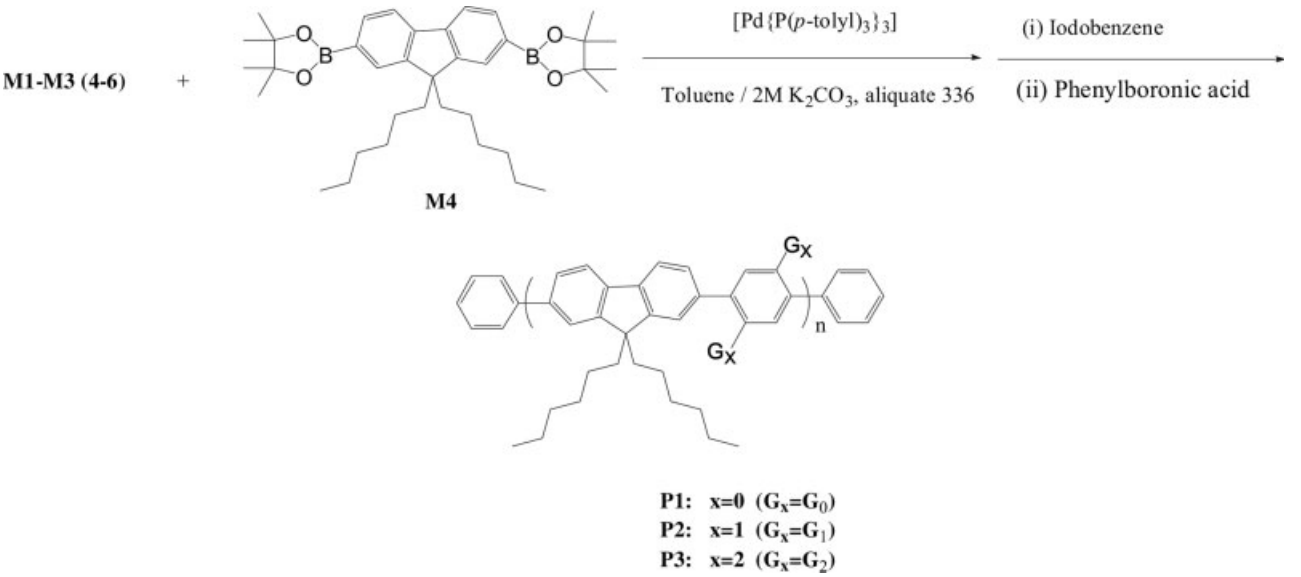

Scheme 2. Synthetic routes of polymers **P1**–**P3**.

6.87–6.98 (broad, 18H), 7.39–7.57 (broad, 22H), 7.88–8.07 (broad, 32H). ELEM. ANAL. Calcd. for $(C_{257}H_{280}N_{16}O_{30})_n$: C, 75.78%; H, 6.93%; N, 5.50%. Found: C, 74.75%; H, 6.91%; N, 5.05%.

RESULTS AND DISCUSSION

Synthesis and Characterization

The synthetic routes of monomers **M1**–**M3** (**4**–**6**) and polymers **P1**–**P3** are shown in Schemes 1 and 2. In the presence of K_2CO_3 in THF at reflux, 2,5-dibromobenzene-1,4-diols were reacted with various generations of corresponding dendrons to obtain monomers **M1**–**M3** (**4**–**6**), which were then copolymerized with **M4** by Suzuki polycondensations (SPCs). In the beginning, when $Pd(PPh_3)_4$ was used as a catalyst precursor, polymer **P3** could not be obtained because of the shielding effect of **M3** on the reactive site, so Pd[P(*p*-tolyl)$_3$]$_3$ seems to be a superior choice in many SPC cases.[30] Freshly prepared Pd[P(*p*-tolyl)$_3$]$_3$ was used as the catalyst precursor[31] with Aliquate 336 as the phase-transfer reagent in a biphasic system (toluene/aqueous K_2CO_3) and gave alternating copolymers **P1**–**P3**. All dendronized polymers could be fully dissolved in common organic solvents, such as methylene chloride, chloroform, toluene, and THF. The molecular weights of the polymers determined by GPC with polystyrene standards are summarized in Table 1. GPC analysis showed that the weight-average molecular weights and polydispersity indices of the dendronized polymers were in the range of 3.3–4.4 $\times$ 10^4 and 1.4–2.4, respectively. The data reveal that the degree of polymerization decreased as the size of the dendritic monomer increased. The same observation was also reported for the synthesis of similar dendronized polymers.[21,23] The

Table 1. Molecular Weights and Thermal Properties of Polymers **P1**–**P3**

Polymer	M_n[a]	M_w[a]	Polydispersity Index[a]	T_g (°C)[b]	T_d (°C)[c]
P1	17,500	42,000	2.4	122	310
P2	24,100	44,300	1.8	94	341
P3	24,000	33,500	1.4	77	353

[a] Number-average molecular weight (M_n) and weight-average molecular weight (M_w) determined by GPC in THF with polystyrene standards (polydispersity index = M_w/M_n).
[b] Glass-transition temperature determined by DSC at a heating rate of 10 °C min^{-1}.
[c] Temperature at 5% weight loss measured by TGA at a heating rate of 20 °C min^{-1} under nitrogen.

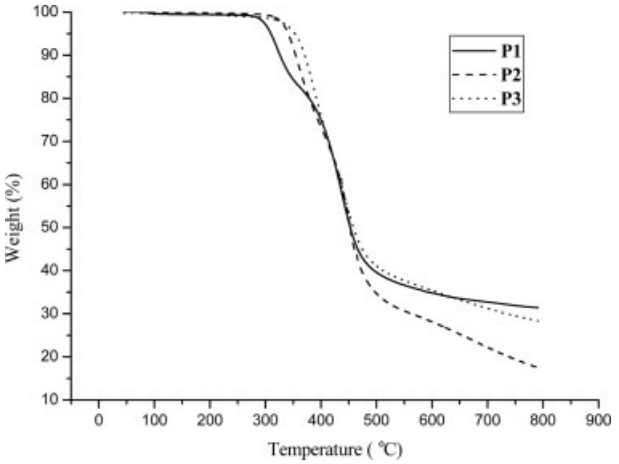

Figure 1. TGA traces of polymers **P1**–**P3**.

thermal properties of the dendronized polymers were investigated with TGA and DSC, and the results are presented in Table 1. All the polymers exhibited good thermal stability: less than 5% weight loss decomposition at about 310–353 °C under nitrogen but more than 50% weight loss decomposition at 450–460 °C (Fig. 1) were observed. The glass-transition temperatures of the dendronized polymers were in the range of 77–122 °C and declined with the increasing size of the attached dendrons. In comparison with a previous report, the glass-transition temperatures of dendronized polymers **P1**–**P3** were higher than that of poly [(9,9-dihexylfluorene)-*alt*-*co*-(2,5-dihexyl-2,5-phenylene)] (glass-transition temperature = 50 °C) or poly[(9,9-dihexylfluorene)-*alt*-*co*-(2,5-dihexyloxy-1,4-phenylene)] (glass-transition temperature = 72 °C).[32]

Optical Properties

The spectroscopic properties of polymers **P1**–**P3** were measured in both solutions (THF) and solid films. The optical properties of polymers **P1**–**P3** are summarized in Table 2. The dendronized polymers showed very similar absorption and emission characteristics in THF. As shown in Figure 2, the polymers in THF solutions exhibited an absorption peak at about 300 nm whose intensity increased with the generation number; this was due to the absorption of the peripheral OXD moieties. This result further confirmed the accomplishment of various generations of OXD dendrimers. The additional absorption peak at about 367 nm was assigned to the π–π^* transition contributed from the conjugated backbones of the polymers, which was not affected by the generation of dendronized polymers. Upon the excitation of the backbones of polymers **P1**–**P3** at 367 nm, the PL emission spectra displayed the maximum intensity at about 414 nm. The PL spectra in THF are almost identical for polymers **P1**–**P3**, as shown in Figure 3. In contrast to dilute solutions (in THF), the absorption spectra of the polymers in solid films are similar (a little redshifted) to those in solutions. The optical band gaps determined from the absorption edges of the UV–vis spectra of polymers **P1**–**P3** in solid films were found to be 3.03 eV. The PL emission spectra of polymers **P1**–**P3** in solid films are only 4–7 nm bathochromically redshifted compared with those in solutions. In particular, because of the stronger aggregation in the solid films of the lowest generation polymer, **P1**, having the smallest dendron size, shows a more obvious shoulder followed by a long, featureless tail (extending into the red region) than the higher generation polymers **P2** and **P3** (Fig. 4). It can be concluded that the higher generation polymers have more site-isolation or dilution effects because of the larger size of the dendrons. A previous publication[33] reported that the various lengths of alkoxy side chains in

Table 2. Absorption and PL Emission Spectral Data of Polymers **P1**–**P3** in THF and Solid Films

Polymer	$\lambda_{abs,sol}$[a] (nm)	$\lambda_{abs,film}$[b] (nm)	Band Gap[c] (eV)	$\lambda_{PL,sol}$[d] (nm)	$\lambda_{PL,film}$[e] (nm)	$Fwhm_{PL,film}$[f] (nm)	$\Phi_{PL,sol}$[g]	$\Phi_{PL,film}$[h]
P1	301,364	323,388	3.03	414	421	44	0.60	0.08
P2	300,367	322,380	3.03	414	421	45	0.87	0.18
P3	300,367	321,376	3.03	415	419	44	0.82	0.26

[a] $\lambda_{abs,sol}$ were defined from the peaks of absorption spectra in solution.
[b] $\lambda_{abs,film}$ were defined from the peaks of absorption spectra in solid films.
[c] Band gaps were calculated from the onsets of UV-visible absorption spectra of **P1–P3** in solid films.
[d] $\lambda_{PL,sol}$ were defined from the peaks of PL spectra in solution.
[e] $\lambda_{PL,film}$ were defined from the peaks of PL spectra in solid films.
[f] $Fwhm_{PL,film}$ were defined from full width at half maximum of PL spectra in solid film.
[g] Solution fluorescence quantum efficiency measured in THF, relative to 9,10-diphenylanthracene ($\Phi_{PL} = 0.90$).
[h] PL quantum efficiency estimated relative to 9,10-diphenylanthracene in poly(methyl methacrylate) as a standard ($\Phi_{PL} = 0.83$).

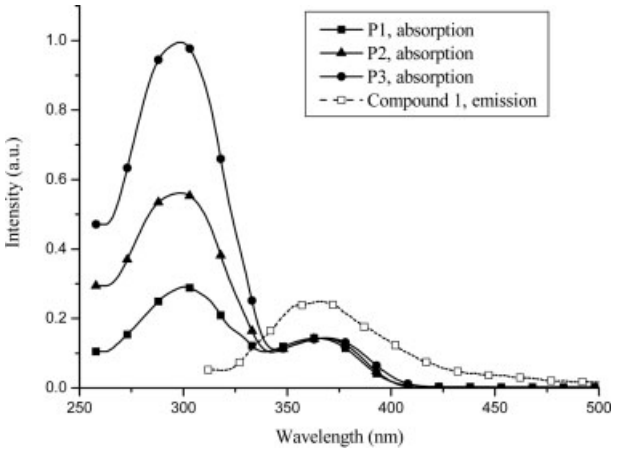

Figure 2. Normalized UV–vis absorption spectra of polymers **P1**–**P3** and PL emission spectrum of compound **1** in THF. The absorption spectra are normalized at the absorption peaks of the polymer backbones around 367 nm.

poly[(9,9-dihexylfluorene)-*alt*-*co*-1,4-phenylene)] (PDHFP) were attached to the phenylene rings of the backbones and that the full width at half-maximum (fwhm) values of these polymers strongly depended on the lengths of the attached alkoxy side chains. The fwhm value decreased from 62 nm in PDHFP (without any side chain on the phenylene ring) to 46 nm in poly(9,9-dihexylfluorene)-(2,5-didecyloxy-1,4-phenylene) (PDHFDDOP) (longer side chains of $-OC_{10}$ on the phenylene ring). The report explained that the smaller fwhm values of the polymers with longer side chains were due to the emission resulting from more isolated main-chain fluorophores. Thus, the fwhm values of the emission curves in solid films of dendronized polymers **P1**–**P3** were also quite narrow (44–45 nm), and purer blue-light emissions were yielded because of their outstanding site-isolation effect. In addition, compared with PDHFP, the vibronic structures in PL emissions of **P2** and **P3** were remarkably reduced, and no noticeable spectral shoulder above 500 nm was observed.

A comparison of the PL emission spectrum of model compound **1** and the absorption spectra of dendronized polymers **P1**–**P3** in THF (Fig. 2) shows that the overlap of the OXD emission peak (363 nm) and **P1**–**P3** backbone absorption peaks (ca. 367 nm) was extremely large. The large spectral overlap between the two interacting chromophores indicates that the probability of donor–acceptor energy transfer should be high. The energy-transfer efficiency of the dendritic wedge is estimated by the intensity ratio of the maximum absorption of OXD dendrons in the absorption spectrum to that in the fluorescence excitation spectrum.[34] According to this estimation, the energy-transfer efficiencies of various generations of OXD dendrons were 59, 43, and 49% for **P1**, **P2**, and **P3**, respectively. It was consistently found that the energy-transfer efficiency decreased as the generation (i.e., the size) of the surface-functionalized poly(benzyl ether)-type dendritic wedge increased. Upon excitation at either OXD dendrons or polymer backbones of polymers **P1**–**P3** in THF, the obtained PL emission spectra are identical, as shown in Figure 5(a). The almost complete disappearance of the OXD emission at 363 nm indicates that energy-transfer efficiency was extremely high in these molecules. A comparison of the PL emission intensity from the sensitized excitation (excited at the maximum absorption of OXD dendrons) and that from the direct

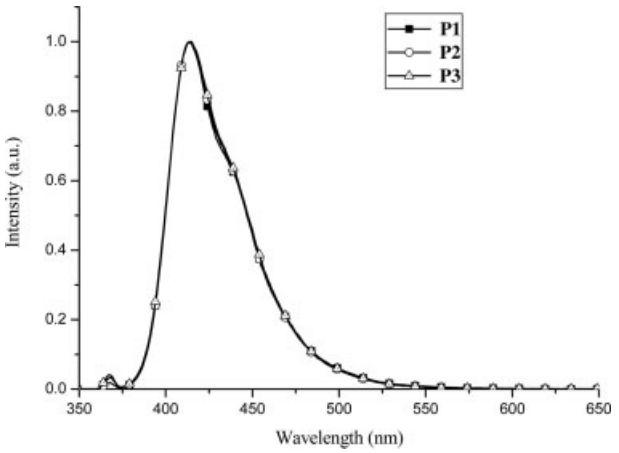

Figure 3. Normalized PL spectra of polymers **P1**–**P3** in THF.

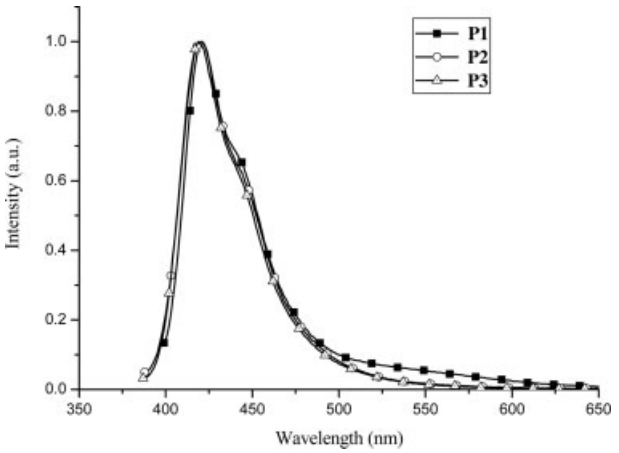

Figure 4. Normalized PL spectra of polymers **P1**–**P3** in solid films.

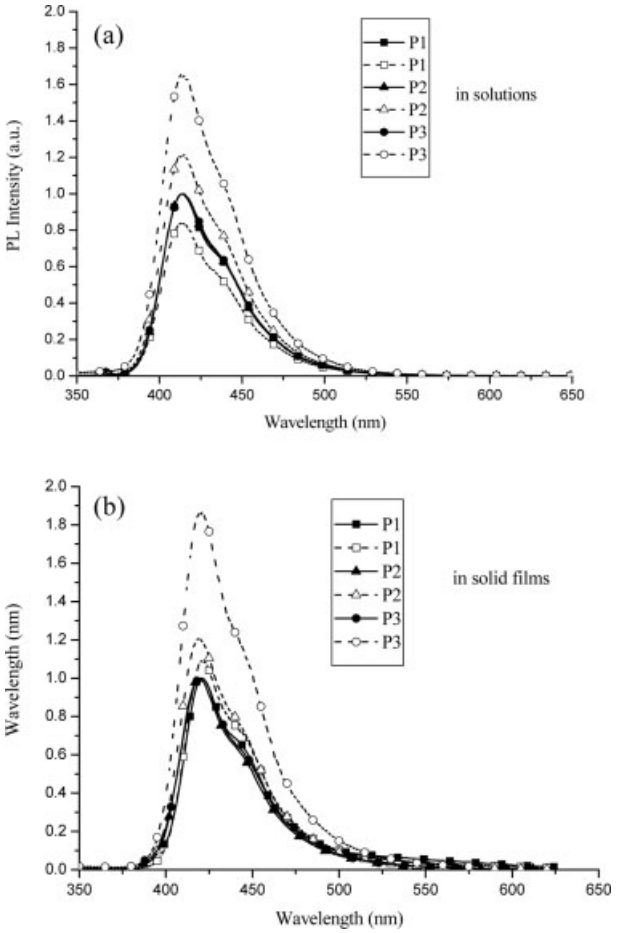

Figure 5. PL emission spectra of polymers **P1**–**P3** (a) in solutions (THF) and (b) in solid films, which were excited at the maximum absorption of the polymer backbones (solid symbols) and the polymer-periphery OXD dendrons (open symbols).

excitation (excited at the maximum absorption of the polymer backbones) of dendronized polymers **P2** and **P3** shows more intense PL backbone emissions by the sensitized excitation from the energy transfer of OXD dendrons than by the direct excitation from the absorption of chromophore backbones. This indicates that the overall fluorescence of dendronized polymers **P1**–**P3** resulted not only from the contribution of the polymer backbones but also from that of the peripherally dendritic OXD units. In addition, the OXD-functionalized dendritic wedges were very efficient light-harvesting moieties for funneling energy to the polymer backbones. As shown in Figure 5(b), the excitations of the peripheral OXD moieties of dendronized polymers **P1**–**P3** in solid films resulted in fluorescence patterns similar to those excited at the maximum absorption of the polymer backbones alone. In particular, the PL emission intensities by the sensitized excitations of OXD dendrons in solid films of polymers **P1**–**P3** were all stronger than those by the direct excitations of their polymer conjugated backbones. Actually, the PL emission intensity of polymer **P3** in a solid film excited at peripheral OXD dendrons was about 86% higher than that excited at the backbones. In general, similar effects have been commonly described for dye-labeled dendrimers.[35–38] However, the result demonstrates that dendronized polymers may show stronger emissions through efficient energy transfer from peripheral dendrons to emitting backbones.

As listed in Table 2, the PL quantum yields of polymers **P1**–**P3** in THF solutions were measured with 9,10-diphenylanthracene as a reference standard[39] (cyclohexane, PL quantum yield = 0.9), and the highest quantum yield reached 0.87. The PL quantum yields in solid films were measured with the same standard in poly(methyl methacrylate).[40] The shielding effect of the dendritic side chains on the polymer backbones was also reflected in the emission efficiency of the

Table 3. HOMO and LUMO Energies and Electrochemical Properties of Polymers **P1**–**P3**

Polymer	$E^{red/onset}$ (V)[a]	$E^{red/peak}$ (V)[b]	$E^{ox/onset}$ (V)[a]	E^{HOMO} (eV)[c]	E^{LUMO} (eV)[c]	E_g (eV)[d]
P1	−2.07	−2.57	0.93	−5.73	−2.73	3.00
P2	−2.01	−2.58	0.94	−5.74	−2.79	2.95
P3	−2.03	−2.54	0.93	−5.73	−2.77	2.96

[a] $E^{red/onset}$ and $E^{ox/onset}$ were determined from the intersection of two tangents drawn at the rising and background currents of the CV measurements.
[b] $E^{red/peak}$ was defined from the first peak in the cathodic sweep.
[c] E^{HOMO} and E^{LUMO} of polymers were estimated with regard to the energy level of the ferrocene reference (4.8 eV below the vacuum level).
[d] Optical band gap.

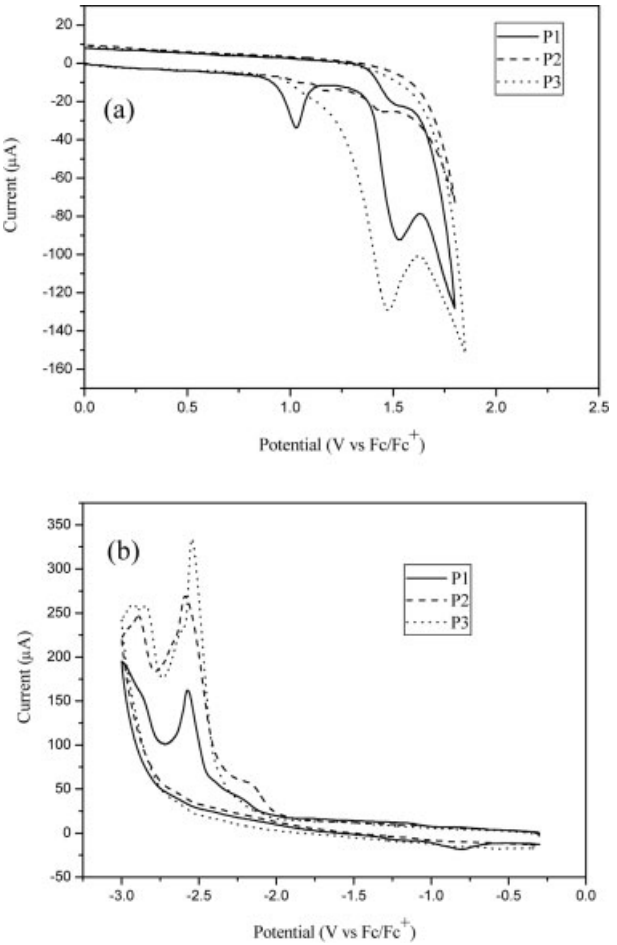

Figure 6. Cyclic voltammetry of polymers **P1**–**P3** during (a) the oxidation processes and (b) the reduction processes.

dendronized polymers. Although this relative method could give only an estimation of the fluorescence quantum yields of the polymers, the data still indicated that the fluorescence quantum yields of the polymers depended on the sizes of the attached dendrons; that is, the larger the dendrons were, the higher the PL quantum yields were. Therefore, the second generation of dendronized polymer **P3** in the solid film showed the highest quantum yield, which was attributed to the minimization of the self-quenching by the attachment of bulky pendent dendrons onto the polymer backbones.

Electrochemical Properties

Cyclic voltammetry measurements were carried out to determine the energies of the highest occupied molecular orbital (HOMO) and lowest unoccupied molecular orbital (LUMO) of polymers **P1**–**P3**. The HOMO, LUMO, and electrochemical properties of the polymers are summarized in Table 3. As shown in Figure 6, polymers **P1**–**P3** showed almost identical behavior during anodic and cathodic scans because of the same backbone structure of poly(fluorene-*co*-*alt*-phenylene) with different generations of OXD dendrons. In the cyclic voltammogram of polymer **P1**, the difference between the anodic and cathodic onset potentials was 3.00 V, which implied that the π–π^* band gap of the polymer was 3.00 eV. The data were similar to those obtained from the absorption edge of the UV–vis spectrum. With respect to the energy level of the ferrocene reference (4.8 eV below the vacuum level),[41] the HOMO and LUMO energy levels of polymer **P1** were estimated to be −5.73 and −2.73 eV, respectively.

CONCLUSIONS

A series of novel poly(fluorene-*co*-*alt*-phenylene)s containing different generations of dendronized side chains, including Fréchet-type poly(aryl ether) dendrons and functional peripheral OXD groups, were synthesized. The resulting polymers possessed good thermal stability and excellent solubility in common organic solvents. The emission spectral quality (narrow fwhm and reduced tail) could be improved by the insertion of bulky OXD dendrons as side chains of the polymers because of less molecular close stacking. In addition, it was demonstrated that the peripheral OXD dendrons had specific light-antenna and enhanced backbone luminescence properties. The PL emission intensities by the sensitized excitations of OXD dendrons in solid films of polymers **P1**–**P3** were all stronger than those by the direct excitations of their polymer conjugated backbones.

The authors thank the National Science Council of Taiwan (Republic of China) for its financial support through NSC 93-2113-M-009-011. Yu-Chie Chen (matrix-assisted laser desorption/ionization time-of-flight mass spectrometry) and Ching-Fong Shu (gel permeation chromatography and cyclic voltammetry measurements) at the Department of Applied Chemistry of National Chiao Tung University (Taiwan) are also acknowledged for their instrumental support.

REFERENCES AND NOTES

1. Tang, C. W.; Vanslyke, S. A. Appl Phys Lett 1987, 51, 913.
2. Shen, Z.; Burrows, P. E.; Bulović, V.; Forrest, S. R.; Thompson, M. E. Science 1997, 276, 2009.

3. Song, S. Y.; Jang, M. S.; Shim, H. K.; Song, I. S.; Kim, W. H. Synth Met 1999, 102, 1116.
4. Peng, Z.; Bao, Z.; Galvin, M. E. Adv Mater 1998, 10, 680.
5. Zhan, X. W.; Liu, Y. Q.; Wu, X.; Wang, S.; Zhu, D. B. Macromolecules 2002, 35, 2529.
6. Chen, Z. K.; Meng, H.; Lai, Y. H.; Huang, W. Macromolecules 1999, 32, 4351.
7. Bao, Z.; Peng, Z.; Galvin, M. E.; Chandross, E. A. Chem Mater 1998, 10, 1201.
8. Chung, S. J.; Kwon, K. Y.; Lee, S. W.; Jin, J. I.; Lee, C. H.; Lee, C. E.; Park, Y. Adv Mater 1998, 10, 1112.
9. Wu, F. I.; Reddy, D. S.; Shu, C. F.; Liu, M. S.; Jen, A. K. Y. Chem Mater 2003, 15, 269.
10. Shu, C. F.; Dodda, R.; Wu, F. I.; Liu, M. S.; Jen, A. K. Y. Macromolecules 2003, 36, 6698.
11. Lee, D. W.; Kwon, K. Y.; Jin, J. L.; Park, Y.; Kim, Y. R.; Hwang, I. W. Chem Mater 2001, 13, 565.
12. Kim, J. H.; Park, J. H.; Lee, H. Chem Mater 2003, 15, 3414.
13. (a) Sung, H. H.; Lin, H. C. Macromolecules 2004, 37, 7945; (b) Sung, H. H.; Lin, H. C. J Polym Sci Part A: Polym Chem 2005, 43, 2700; (c) Jin, S. H.; Kim, M. Y.; Kim, J. Y.; Lee, K.; Gal, Y. S. J Am Chem Soc 2004, 126, 2474.
14. (a) Pan, J.; Zhu, Zhu, W.; Li, S.; Zeng, W.; Cao, Y.; Tain, H. Polymer 2005, 46, 7658; (b) Pan, J.; Zhu, W.; Li, S.; Xu, J.; Tian, H. Eur J Org Chem 2006, 986; (c) Du, P.; Zhu, W. H.; Xie, Y. Q.; Zhao, F.; Ku, C. F.; Cao, Y.; Chang, C. P.; Tian, H. Macromolecules 2004, 37, 4387; (d) Tseng, Y. H.; Wu, F. I.; Shih, P. I.; Shu, C. F. J Polym Sci Part A: Polym Chem 2005, 43, 5147.
15. Bernius, M. T.; Inbasekaran, M.; O'Brien, J.; Wu, W. W. Adv Mater 2000, 12, 1737.
16. Grice, A. W.; Bradley, D. D. C.; Bernius, M. T.; Inbasekaran, M.; Wu, W. W.; Woo, E. P. Appl Phys Lett 1998, 73, 629.
17. Redecker, M.; Bradley, D. D. C.; Inbasekaran, M.; Woo, E. P. Appl Phys Lett 1998, 73, 1565.
18. Millard, I. S. Synth Met 2000, 111, 119.
19. Setayesh, S.; Grimsdale, A. C.; Weil, T.; Enkelmann, V.; Müllen, K.; Meghdadi, F.; List, E. J. W.; Leising, G. J Am Chem Soc 2001, 123, 946.
20. Pogantsch, A.; Wenzl, F. P.; List, E. J. W.; Leising, G.; Grimscale, A. C.; Müllen, K. Adv Mater 2002, 14, 1061.
21. Marsitzky, D.; Vestberg, R.; Blainey, P.; Tang, B. T.; Hawker, C. J.; Carter, K. R. J Am Chem Soc 2001, 123, 6965.
22. Tang, H. Z.; Fujiki, M.; Zhang, Z. B.; Torimitsu, K.; Motonaga, M. Chem Commun 2001, 2426.
23. Chou, C. H.; Shu, C. F. Macromolecules 2002, 35, 9673.
24. Fu, Y. Q.; Li, Y.; Li, J.; Yan, S.; Bo, Z. S. Macromolecules 2004, 37, 6395.
25. Kreyenschmidt, H.; Kaerner, G.; Fuhrer, T.; Ashenhurst, J.; Karg, S.; Chen, W. D.; Lee, V. Y.; Scott, J. C.; Miller, R. D. Macromolecules 1998, 31, 1099.
26. Klärner, G.; Davey, M. H.; Chen, W. D.; Scott, J. C.; Miller, R. D. Adv Mater 1998, 10, 993.
27. (a) Liu, B.; Yu, W. L.; Lai, Y. H.; Huang, W. Chem Mater 2001, 13, 1984; (b) Mikroyannidis, J. A. J Polym Sci Part A: Polym Chem 2006, 44, 4015.
28. Wu, C. W.; Tsai, C. M.; Lin, H. C. Macromolecules 2006, 39, 4298.
29. Ranger, M.; Rondeau, D.; Leclerc, M. Macromolecules 1997, 30, 7686.
30. (a) Frahn, J.; Karakaya, B.; Schäfer, A.; Schlüter, A. D. Tetrahedron 1997, 53, 15459; (b) Schlüter, S.; Frahn, J.; Schlüter, A. D. Macromol Chem Phys 2000, 201, 139.
31. Tolman, C. A.; Seidel, W. C.; Gerlach, D. H. J Am Chem Soc 1972, 94, 2669.
32. Tokito, S.; Tanaka, H.; Noda, K.; Okada, A.; Taga, Y. Appl Phys Lett 1997, 70, 1929.
33. Zeng, G.; Yu, W. L.; Chua, S.; Huang, W. Macromolecules 2002, 35, 6907.
34. Haugland, R. P.; Yguerabide, J.; Stryer, L. Proc Natl Acad Sci USA 1969, 63, 23.
35. Adronov, A.; Gilat, S. L.; Fréchet, J. M. J.; Ohta, K.; Neuwahl, F. V. R.; Fleming, G. R. J Am Chem Soc 2000, 122, 1175.
36. Adronov, A.; Malenfant, P. R. L.; Fréchet, J. M. J. Chem Mater 2000, 12, 1463.
37. Weil, T.; Reuther, E.; Müllen, K. Angew Chem Int Ed 2002, 41, 1900.
38. Du, P.; Zhu, W. H.; Xie, Y. Q.; Zhao, F.; Ku, C. F.; Cao, Y.; Chang, C. P.; Tian, H. Macromolecules 2004, 37, 4387.
39. Eaton, D. Pure Appl Chem 1998, 60, 1107.
40. Practical Fluorescence; Guilbault, G. G., Ed.; Marcel Dekker: New York, 1990; Chapter 1.
41. Pommerehne, J.; Vestweber, H.; Guss, W.; Mahrt, R. F.; Bässler, H.; Porsch, M.; Daub, J. Adv Mater 1995, 7, 551.